Secular Deformation in Southern Cascadia: Elastic Modeling as Informed by Geodetic Observation

Jason R. Patton[1,2], Chris Rollins[3], Robert C. McPherson[1], Mark Hemphill-Haley[1], Todd Williams[2], Thomas H. Leroy[2,4]
Humboldt State University, Dept. of Geology, 2. Cascadia GeoSciences, 3. Michigan State University, 4. Pacific Watershed Associates
Department of Earth and Environmental Sciences
MICHIGAN STATE UNIVERSITY

Abstract

Northwestern California is sheared over time by deformation along the Cascadia megathrust, the northern San Andreas fault, and subsidiary faults. We use geodetic data and modeling to shed light on the earthquake cycle and seismic hazard in this region. We synthesize tide gage, benchmark survey, and GPS data to document 20th-21st century rates of vertical land motion. These rates (corrected for glacial isostatic adjustment) range from -5 mm/yr in southern Humboldt Bay to +2 mm/yr near Crescent City. Subsidence in Humboldt Bay is apparent in all three datasets and may suggest downwarping of the surface above a local locked patch on the megathrust, motion on upper-plate faults, or possible anelastic/nontectonic processes.

We explore these possibilities using the new Slab2.0 Cascadia geometry and inverse methods that combine these uplift rates with horizontal GPS velocities corrected for locking on the San Andreas. We also examine how the earthquake cycle on these faults would affect the local land surface.

Uniform-slip models with the Slab2.0 geometry suggest a Cascadia earthquake rupturing from the trench to 35 km depth (located ~75 km inboard of the coast) would uplift Humboldt Bay by ~15% of the slip amount (e.g. ~2 m for 15 m slip), but an earthquake that only ruptured offshore (where existing interseismic models put the highest locking) would instead cause Humboldt Bay to subside by this amount; this is important for coastal infrastructure and tsunami hazard.

We also explore how postseismic viscoelastic relaxation in the mantle wedge and/or below the downgoing slab could modulate these land motions; we find that if this were to mainly occur below the slab, it would contribute modest uplift following the deep-rupture event but could contribute as much as ~200% of the coseismic subsidence following the all-offshore event (e.g. 4 m for 15 m of slip, for a total of 6 m). This may inform interpretations of coastal subsidence in past Cascadia earthquakes.

Cascadia subduction zone

Chaytor et al. (2004)
Nelson et al. (2004)

Plate configuration for the Cascadia subduction zone (CSZ). Juan de Fuca and Gorda plates are subducting northeastwardly oblique beneath the North America plate at ~36 mm/yr in the Humboldt Bay region. Paleoseismic core sites (marine and terrestrial) are plotted as circles.

Vertical Motion: Coseismic vs. Interseismic

Plafker (1972)

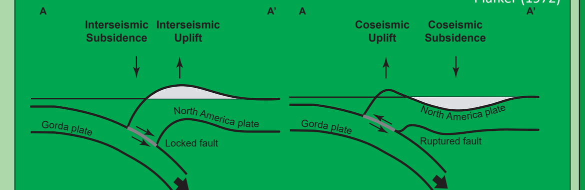

Schematic diagrams showing the pattern of (A) inter-seismic and (B) co-seismic deformation associated with a subduction zone earthquake during an earthquake deformation cycle. Adapted from Plafker (1972) to reflect the spatial pattern of tectonic deformation during the earthquake cycle in Cascadia.

Heterogeneous Coupling

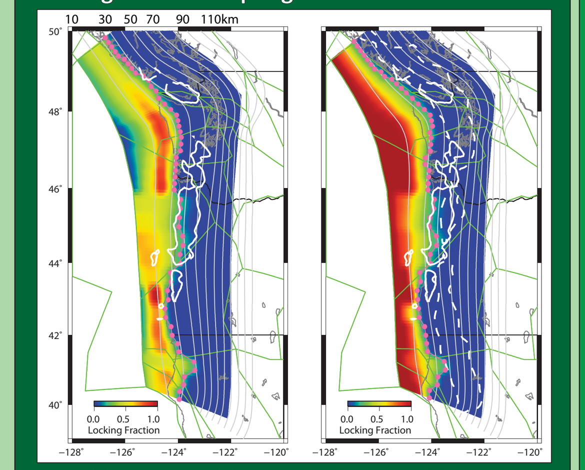

Maps of (A) Gaussian and (B) Gamma decade-scale model locking fraction with pink dotted line that marks the downdip 20% locked contour. Solid white lines mark the 10 mgal gravity anomaly contour of Blakely et al. [2005]. Dashed white line (B) indicates where 96% of tremors are located from the PNSN catalog between 2009 to 2012. Thin gray lines are 10 km depth contours from McCrory et al. [2004] Schmalzle et al., 2014

2. Geodetic Data

Geodetic rates are calculated from tide gage (1977-2018), GPS (~2000-2018), and repeated (1967-1988) benchmark survey data.

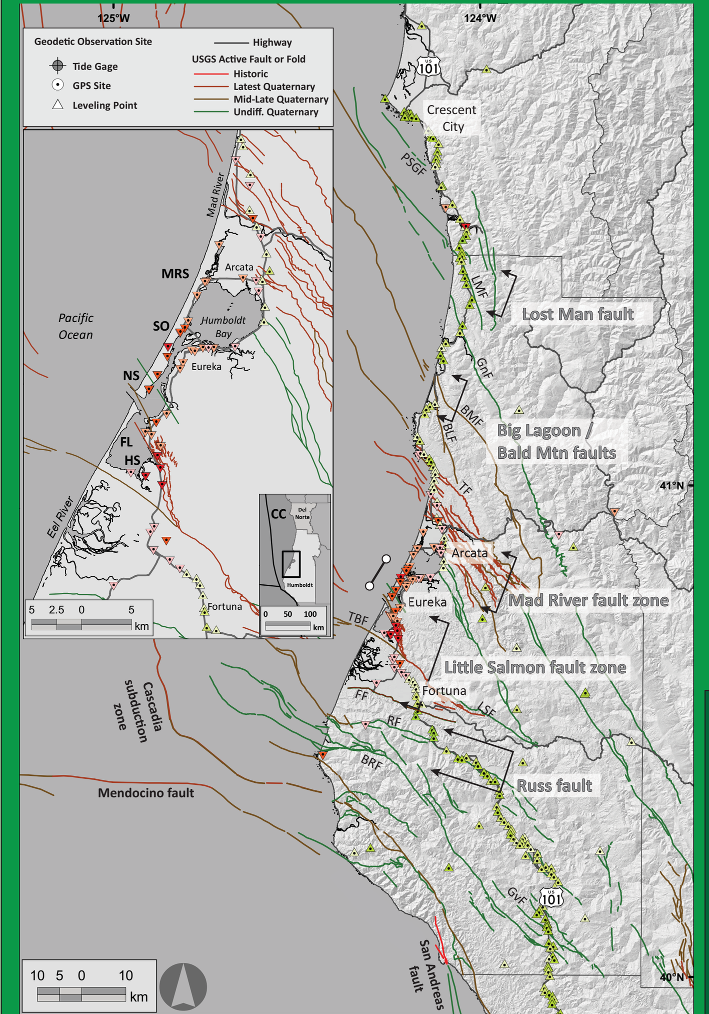

MAP: The map on the left shows the spatial distribution of geodetic sites colored relative to the rate at that site. Green symbols show uplift and red symbols show subsidence. USGS active faults are displayed relative to age of most recent movement.

PROFILES: The profiles show these vertical land motion rates relative to latitude (upper panel) and longitude (lower panel). 1 Sigma uncertainty error bars are shown for sites included in this analysis (gray dots). We highlight geodetic sites that are nearly adjacent to Highway 101 so it makes it easier to visualize the changes in rate with latitude. Sites more distant to the 101 and sites with large uncertainty (e.g. campaign GPS survey data) are plotted as white dots.

1. NAP crustal structures

Active Faulting Associated with the Southern Cascadia Subduction Zone

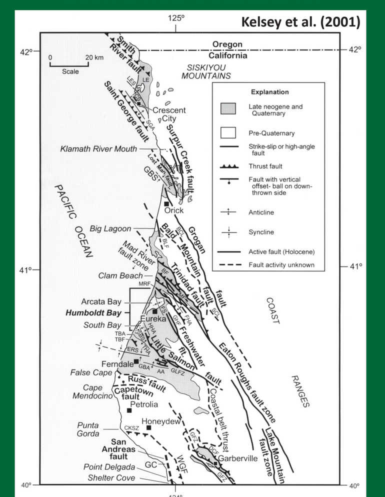

Based on earthquake fault slip-rates and marine terrace uplift-rates, crustal faults in the North America plate may account for between 20% and 30% of the plate convergence in the Humboldt Bay region.

Mad River Fault Zone

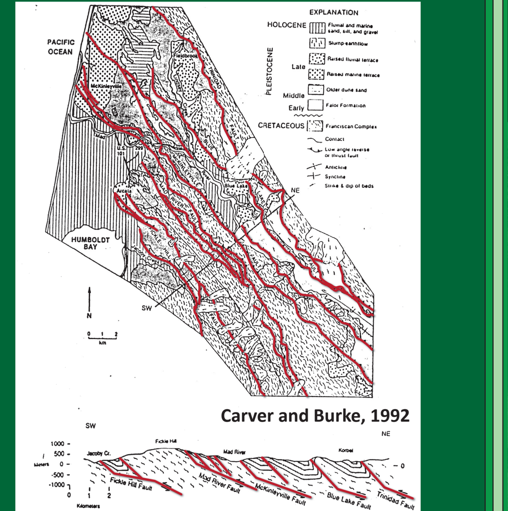

Map and cross-section showing southwest vergent active faults in the Mad River fault zone including the Fickle Hill, Mad River, Mckinleyville, Blue Lake, and Trinidad faults.

3. Lahsāséte Fault

A. Geodetic Evidence

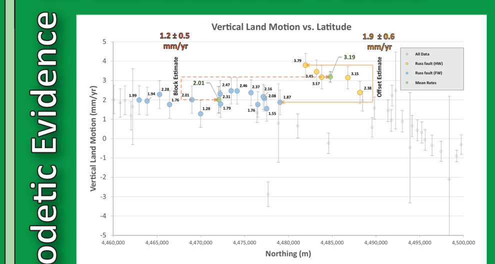

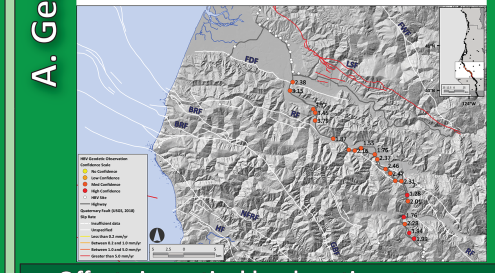

Offsets in vertical land motion rates across active faults in the area are possibly due to strain accumulation across these faults.

We calculate vertical separation rates across these faults in 2 ways: (1) we calculate a rate by differencing the two closest geodetic sites (single offset rate), (2) we calculate the mean block rate on either side of these faults and difference those rates (block rate).

B. Stratigraphic Evidence

Shaded Relief Map of Shively Terraces: Lower terraces T-2, T-3, and T-4 on the left and the upper terrace T-7 on the right. View in Photo A (see below) was acquired in the view directed shown by the yellow arrows. The building in the photo is labeled on the map. Note the anthropogenic modification of the scarp on the left (walls built into the scarp, see photo below). The ends of the scarp in this map are shown as red arrows. Based on the Stallman and Kelsey [2006] incision rate, T-2 is about 18 ky old, T-3 is ~25 ky old, T-4 is ~34 ky old, and T-7 is ~104 ky old.

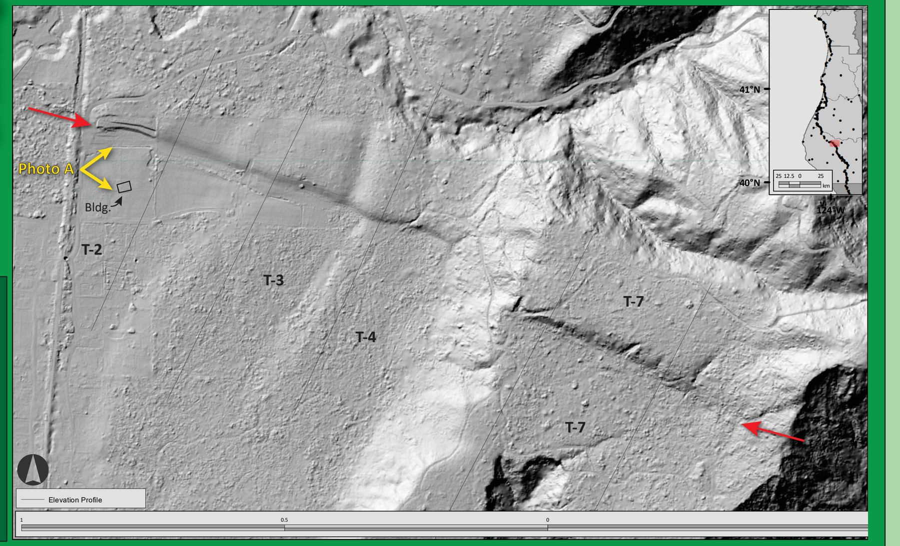

Late Pleistocene Slip Rate: Scarp heights and fault dip are measured using LiDAR data [Dietrich, 2014] and combined with relative ages to calculate slip rates.

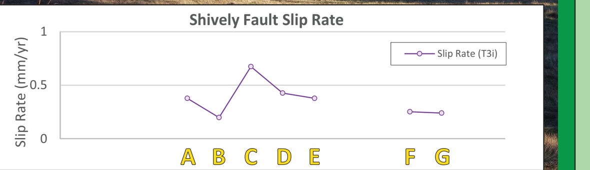

5. Inversion and Backslip Methodology

Geometries of viscoelastic zones in downgoing and overriding plates

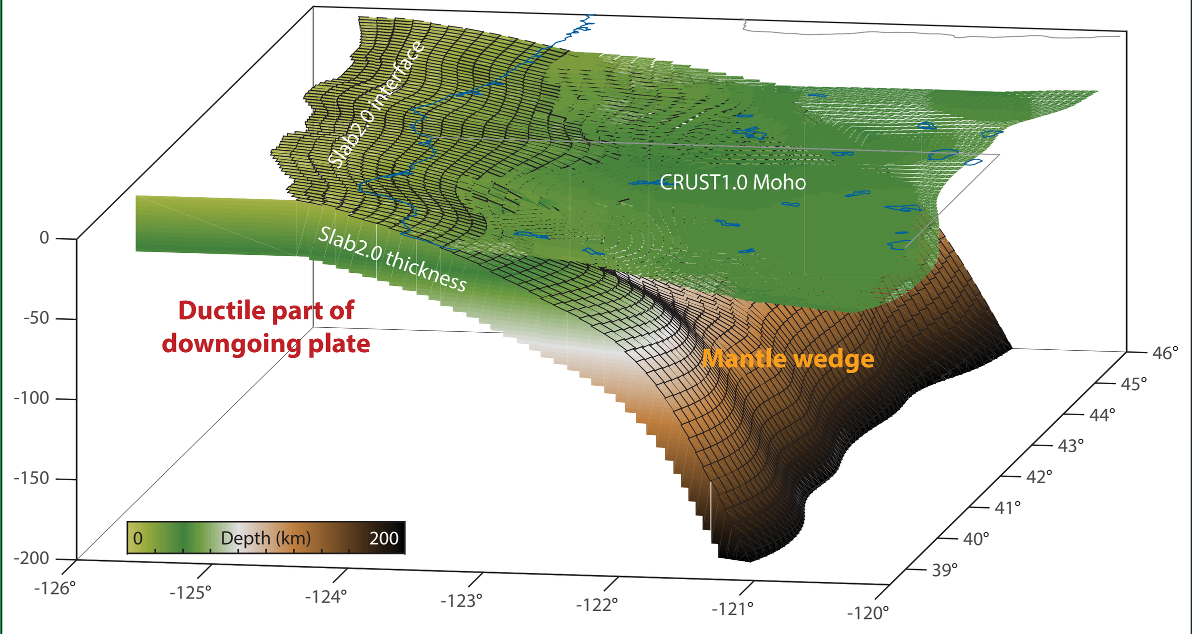

Three Dimensional View: geometry of downgoing Gorda plate. megathrust fault, slab thickness, and Moho. The viscoelastic zone in the downgoing plate extends from a top surface defined by the Slab 2.0 [Hayes et al., 2018] slab depth + slab thickness, down to the base of the model. The viscoelastic zone in the mantle wedge extends from the CRUST1.0 [Laske et al., 2012] Moho down to the Slab2.0 subduction interface.

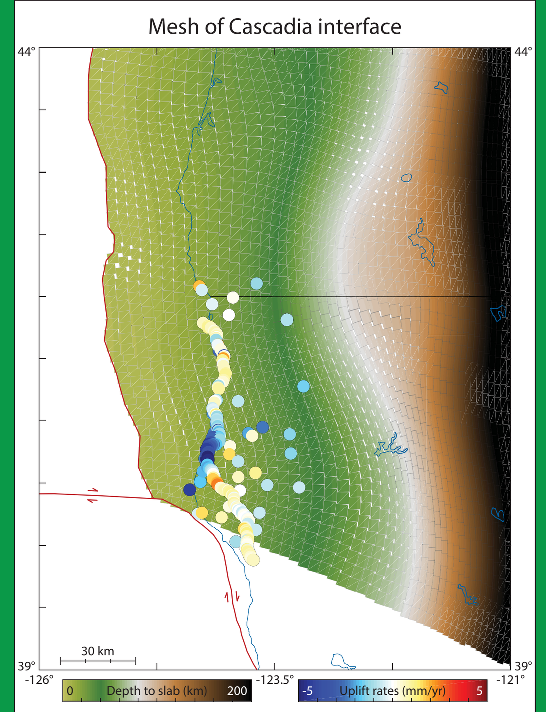

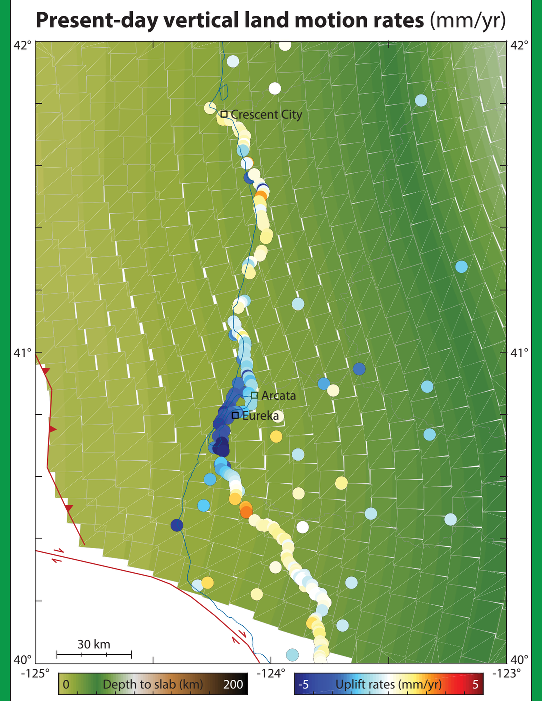

Model Input: 2-D view of fault elements used in this modeling. GPS, tide gage, and benchmark leveling based vertical land motion rate in mm/yr is symbolized as colored dots.

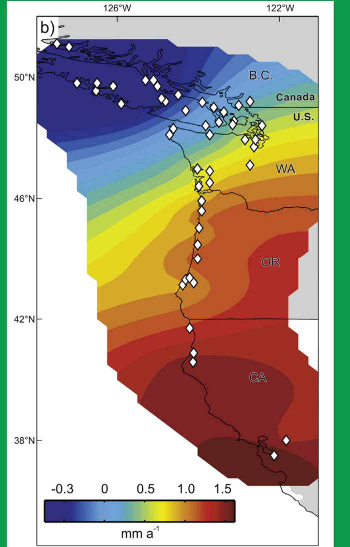

(Engelhart et al., 2015).

GIA Rates: "Late Holocene relative sea-level rise field generated by the empirical-Bayesian spatio-temporal statistical model for the entire study area. This field is subsampled to obtain rates for our individual regions . White diamonds represent all the sites in the database." (from Engelhart et al., 2015). The GIA rate does not vary significantly in the region of our analysis. On the right is a map showing the geodetic rates (plotted above) without GIA correction.

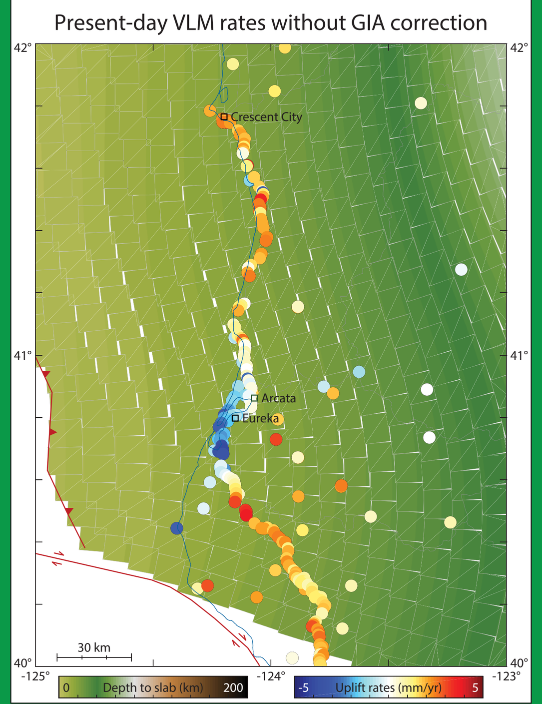

6. Interseismic Results

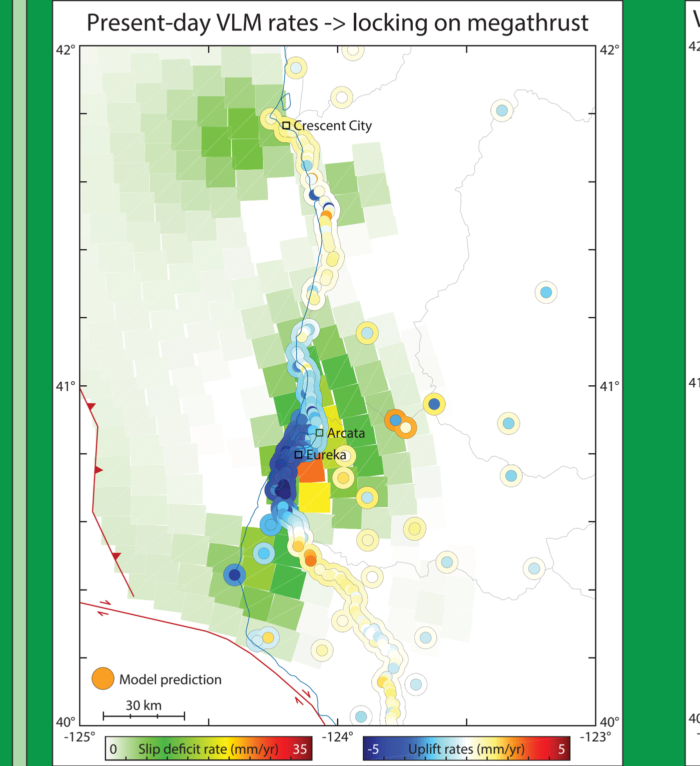

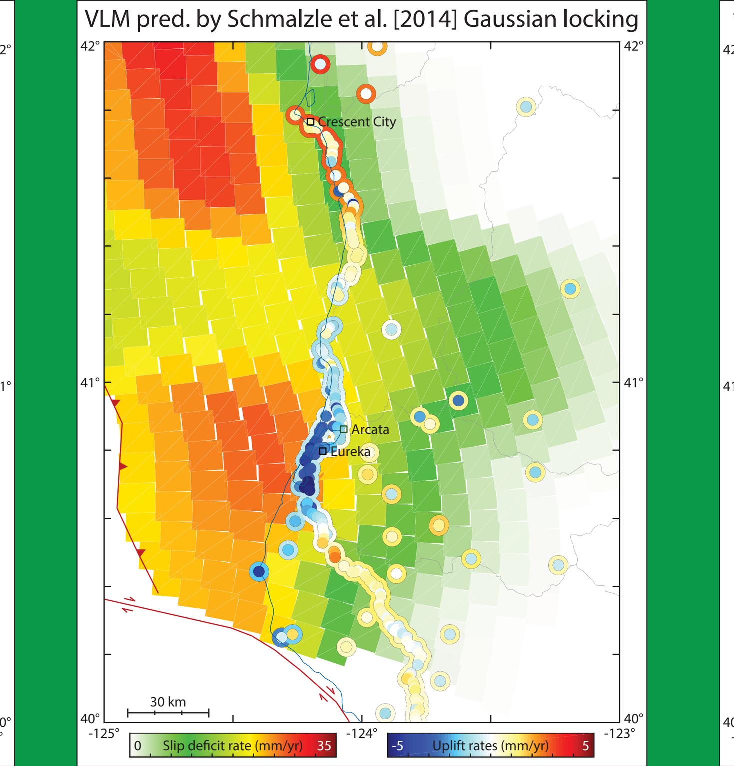

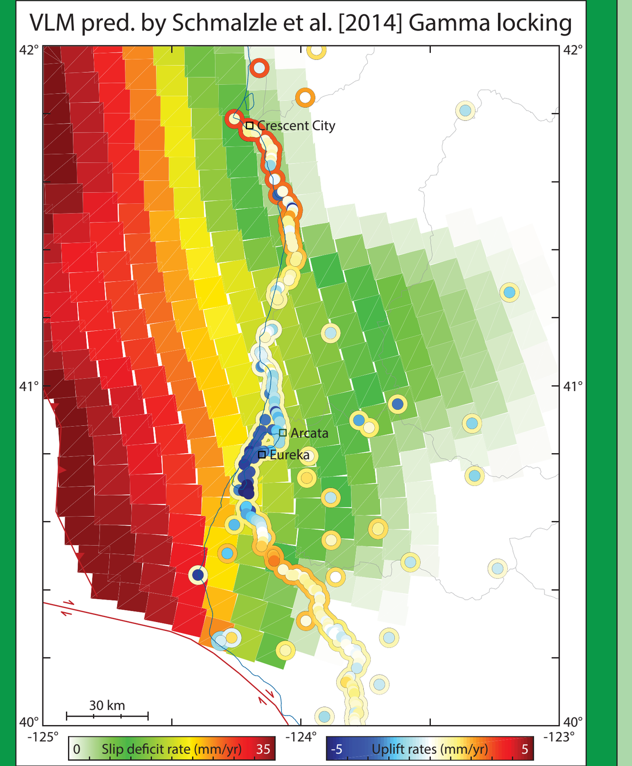

Backslip and VLM Inversion: Slip direction is the average of what is predicted by 6 different Euler poles: those of the three blocks that Schmalzle has coming to the coastline south of the Oregon border (SOCR, ECCR and WCCR), for both the Gaussian and Gamma locking models in Schmalzle et al. [2014] Figure 6. The small circles are the observed VLM rates: the large circles are the model predictions.

VLM rates predicted by Schmalzle et al. [2014] models: These are the present-day VLM rates predicted by the Schmalzle locking models. For each one, we enforce that the slip direction has to be the average of what is predicted by the SOCR, ECCR and WCCR blocks in that model (which have slightly different rotation poles between the Gaussian and Gamma models).

7. Coseismic Results

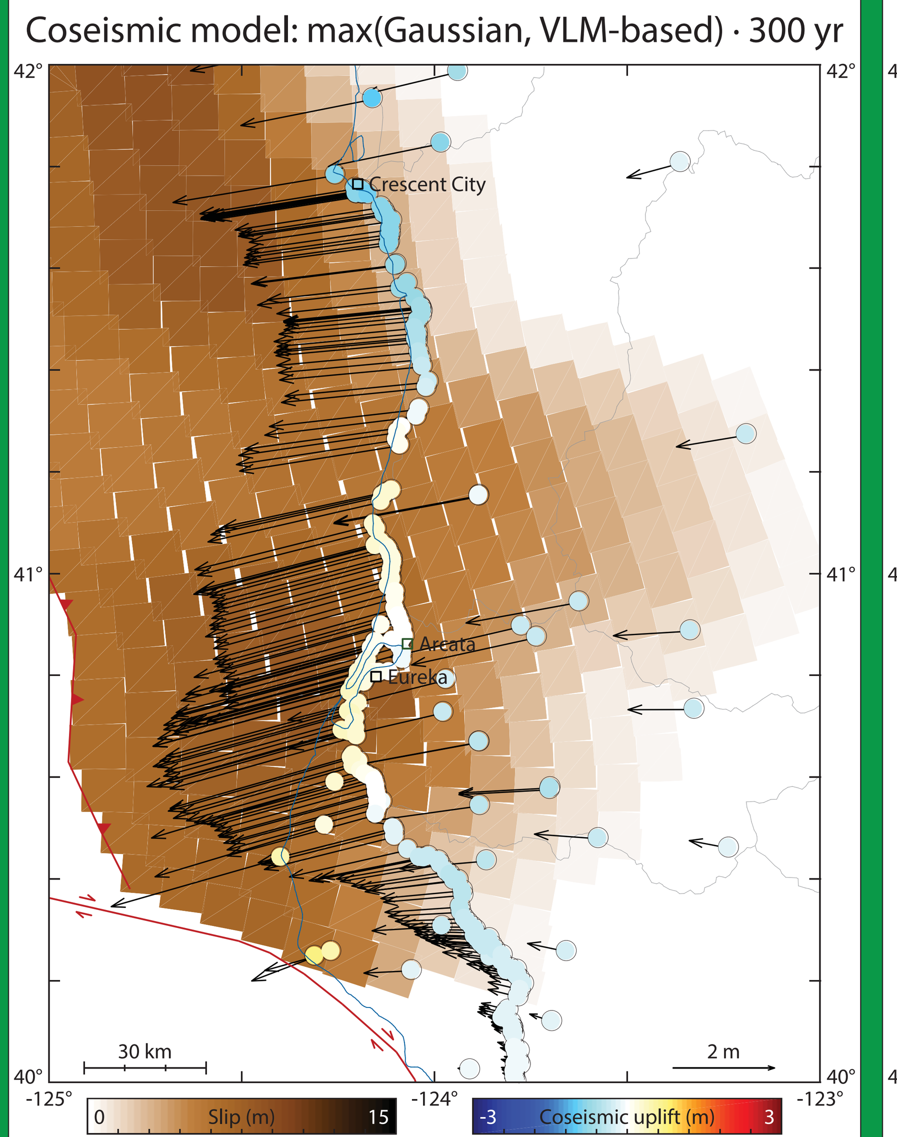

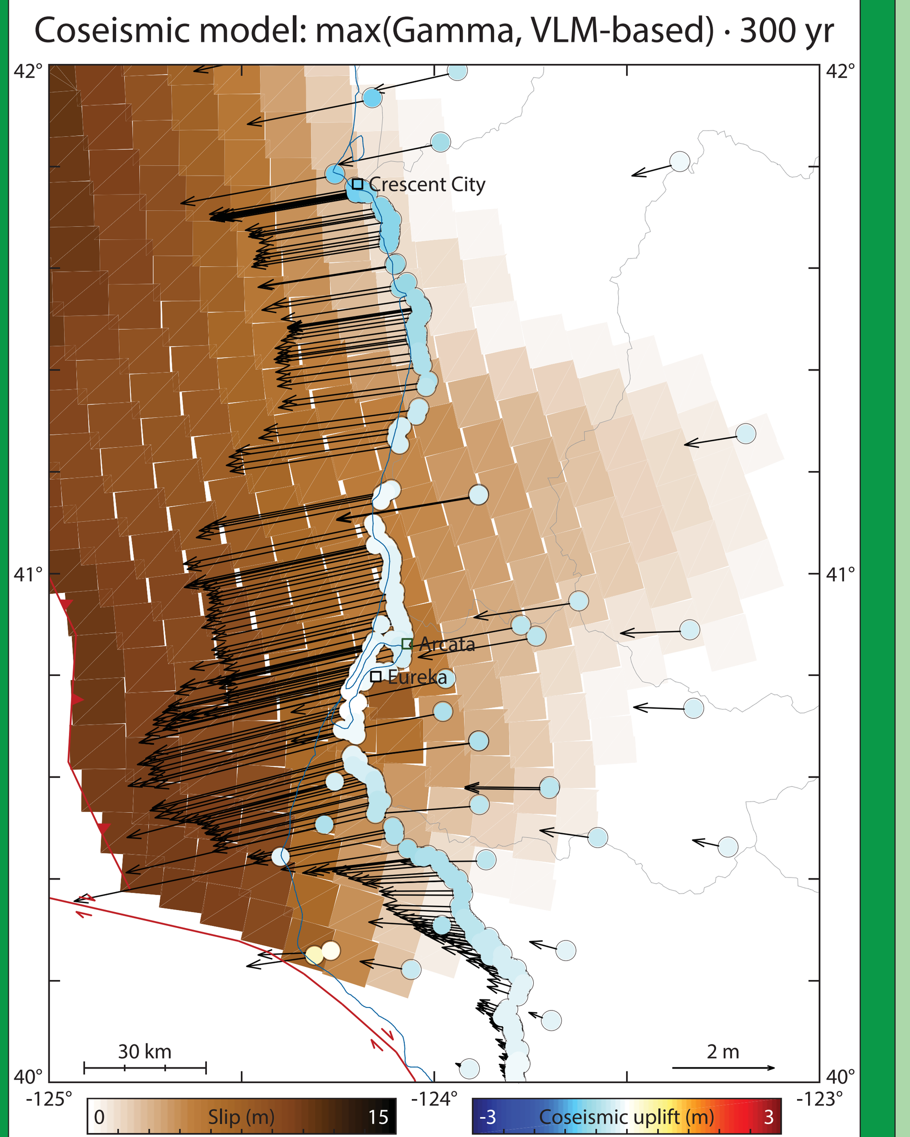

Coseismic models: In each model, we take the maximum of the VLM-inferred interseismic strain accumulation model and the Schmalzle et al. [2014] model indicated. In both cases this adds the additional locked patch under Eureka to the overall Cascadia locking model. We then multiply by -1 (for forward slip) and 300 years (an approximate interseismic interval) to get coseismic slip.

8. Postseismic Results

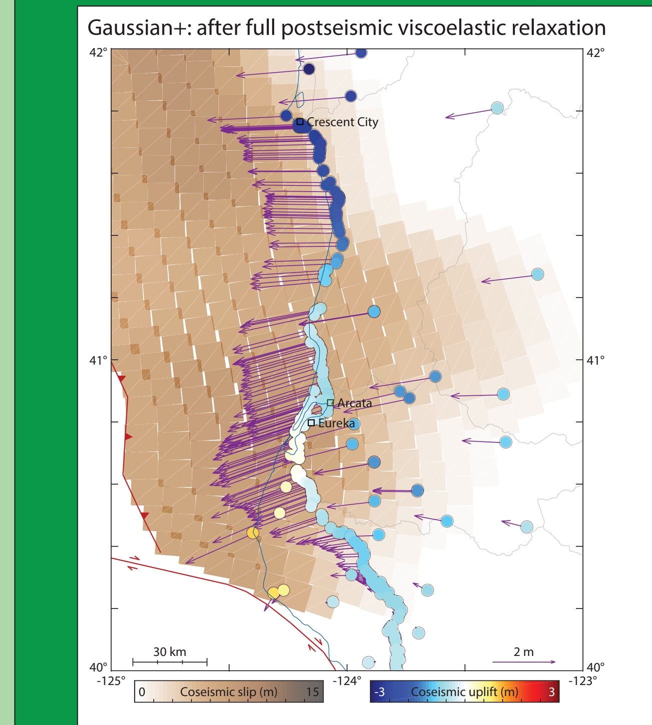

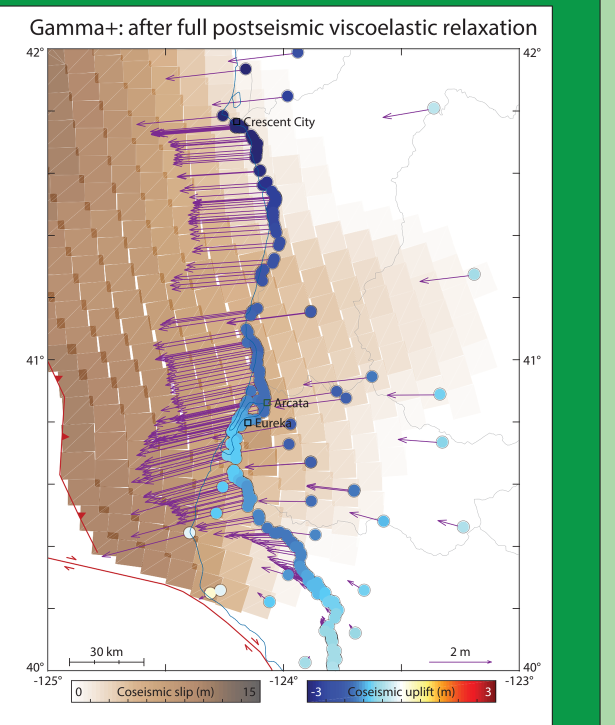

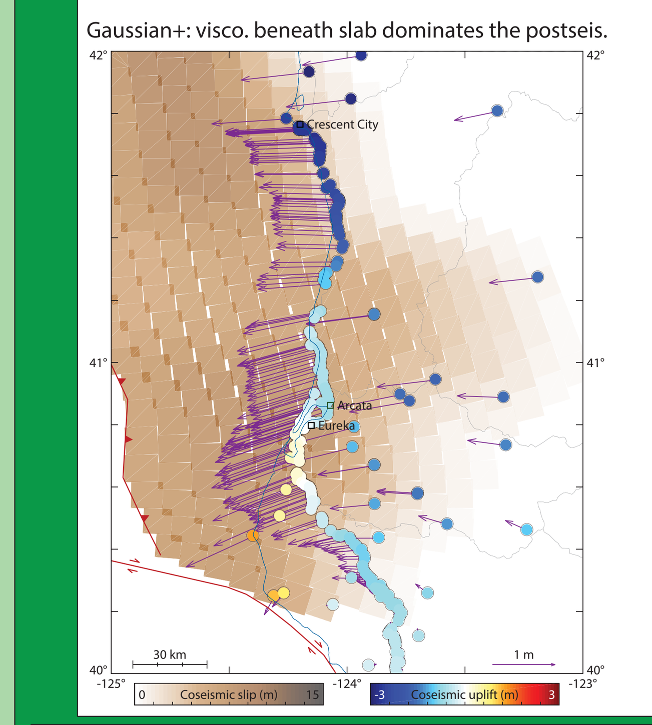

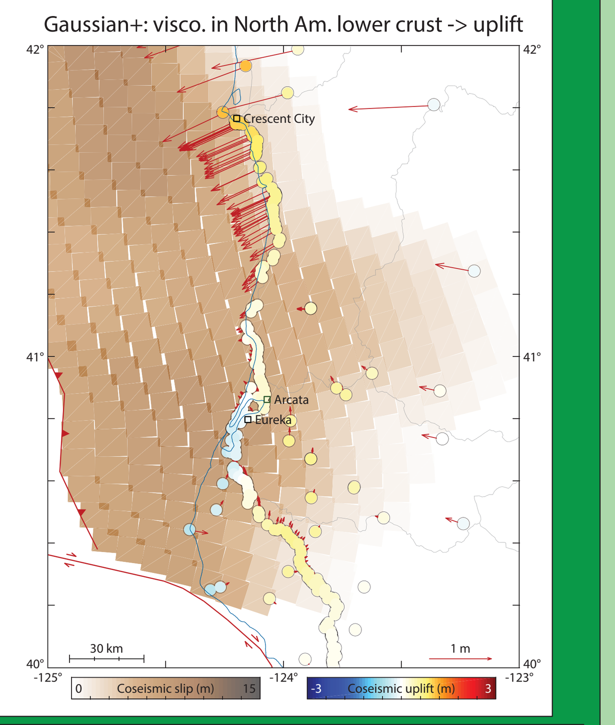

Postseismic Deformation: The top two figures show the cumulative coseismic + postseismic displacements after complete postseismic relaxation in the downgoing Juan de Fuca mantle and overriding North American mantle wedge (geometries in section 5). These models predict multiple meters of additional postseismic subsidence along some areas of the coast. The lower left figure shows the total coseismic + postseismic deformation if one only includes viscoelastic relaxation in the downgoing plate and neglects the overriding mantle wedge. This shows that the downgoing plate actually dominates the simulated postseismic deformation field (as the upper left and lower left figures are nearly identical), with the overriding mantle wedge contributing very little. This is contrary to observations of postseismic deformation in other subduction environments (e.g. Suito and Freymueller, 2009) but perhaps possible as the very young Juan de Fuca plate could have a limited elastic thickness. Not included in the top two models is viscoelastic relaxation in the lower crust of the overriding North American plate (above the mantle wedge). The bottom right figure shows that if this mechanism were present, it could counteract some of the postseismic subsidence that would be predicted by downgoing-plate viscoelastic relaxation.

Take Away Points:

- Interseismic VLM rates can help predict what coseismic and postseismic deformation should be expected in a Cascadia earthquake.
- Don't sleep on the downgoing plate (as far as its importance in the postseismic period). Downgoing-plate viscoelastic relaxation has been observed following the Tohoku earthquake (Sun et al., 2014), and the Juan de Fuca Plate is much younger and perhaps elastically thinner at the trench than the Pacific Plate is in Japan.

Future Work:

- incorporate crustal faults in modeling
- geophysical surveys
- stratigraphic descriptions
- establish chronostratigraphy
- field mapping
- fault trenching

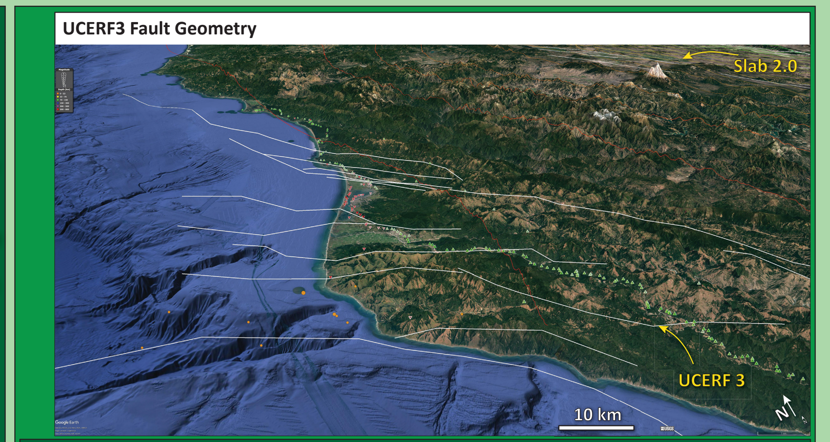

UCERF3 Fault Geometry: Future analyses will incorporate North America crustal faults. We will evaluate the relative contribution of these crustal faults to the regional strain (e.g. Rollins et al., 2018). We hope to determine the spatial extent of different tectonic forcing factors (e.g. where/how do Cascadia, San Andreas, and the Mendocino fault overlap; where are the locii of block boundaries; etc.)